Proceedings of DSCC2019
ASME 2019 Dynamic Systems and Control Conference
October 8-11, 2019, Park City, USA

DSCC2019-9220

DISTRIBUTED CONTROL OF A PLANAR DISCRETE ELASTIC ROD MODEL FOR CATERPILLAR-INSPIRED LOCOMOTION

Helene Nguewou-Hyousse
Department of Electrical Engineering
University of Maryland
College Park, MD 20742
Email: hnguewou@umd.edu

William L. Scott
Department of Aerospace Engineering
and Institute for Systems Research
University of Maryland
College Park, MD 20742
Email: wlscott@umd.edu

Derek A. Paley
Department of Aerospace Engineering
and Institute for Systems Research
University of Maryland
College Park, MD 20742
Email: dpaley@umd.edu

ABSTRACT

During crawling, a caterpillar body stretches and bends, and a wave repeatedly travels from the tail to the head. Recently, caterpillar locomotion has been modeled using the theory of planar discrete elastic rods (PDER). This work takes a similar modeling approach and introduces feedback control laws with communication between neighboring segments. Caterpillar locomotion is modeled first as a network of spring-mass-dampers connected through nearest neighbor interactions and then as a network of linked torsional springs. Feedback laws are designed to achieve consensus and traveling wave solutions. Simulation results show the displacement of each segment of a caterpillar during locomotion. These results show promise for the design of feedback control laws in a network model of soft robotic systems.

INTRODUCTION

Caterpillars are soft-bodied animals that can maneuver in complex three-dimensional environments. Their high deformability allows them to bend, twist, and stretch: a caterpillar can cantilever over a gap that is 90% of its body length [1, 2]. Caterpillars are a good example of distributed control of movements: during a crawling cycle, a wave propagates from tail to head through the coordination of concatenated segments [1, 2]. These segments are lifted and compressed in a damped motion utilizing the storage and release of energy [1].

Caterpillar–inspired soft robots should be able to adapt to small, confined spaces and irregular terrain. They may also be safe when operated alongside humans because their contact force is lessened due to their flexibility [3]. In addition, a soft robot replicating the motion control of a caterpillar should be highly scalable, because their crawling gait does not change despite the mass increase during their life cycle [2]. As such, the applications of a caterpillar-inspired soft robot range from search and rescue to exploration and medicine [4, 5].

Although soft robots inspired by organisms without a skeleton may be easier to design than vertebrate-inspired robots because of the simplicity of their anatomy [6], their deformability may translate into high degrees of freedom. Caterpillar-inspired soft robots have been designed using modular [1, 2, 7, 8], continuum [9, 10, 11], and combined approaches [12]. Wang et al. [7] used a kinematic approach to design a flexible modular robot consisting of joints and solenoid-activated sucker vacuum, controlled by pulse width modulation (PWM). Another robot, Softbot [1, 2], is made of highly elastic silicone rubber and displays a pressurized inside chamber to regulate stiffness. It uses discrete group of shape memory alloy (SMA) springs as actuators, controlled by a pulsed current source driven by a master oscillator, coupled to a second oscillator to generate square waves. Umedachi [9] describes embedded SMA coils along the continuous body axis in the design of a caterpillar-inspired soft robot that employs variation between high and low friction to create adaptive and versatile motion. The friction resulting from the radius of curvature of the robot is controlled by retrograde waves with phase gaps. GoQBot is a SMA-actuated silicone soft robot

with electric wires embedded in two actuators segments for anterior and posterior flexion, and controlled by fixed voltage signal [12]. Finally, optomechanical liquid crystalline elastomer (LCE) material was used to generate and control a traveling wave using spatially modulated light field creating sequential illumination [10, 11].

Although most soft robots show flexibility, adaptability and, in some cases, are capable of more than one locomotion gait, it is difficult to model their dynamics because of the high complexity of their motion and the number of degrees of freedom required. Additionally, they lack a closed-loop control system that can add resilience to the system. Such closed-loop control can be achieved by taking into account sensory feedback.

Prior work on modeling locomotion in a caterpillar-like soft body used inverse-dynamics to represent a planar extensible-link model [13], lumped-mass dynamic model coupled with a control law for gait optimization [14, 15], or electric oscillators dynamics model with closed-loop control [16]. Umedachi's work proposed autonomous decentralized control as a solution to generating and controlling local and adaptive locomotion in soft robots [17,18]. In particular, they applied autonomous decentralized control to modular sections of a 3D printed robot to induce locomotion through phase gradient [18]. Prior work in the area of collective motion of a network of oscillators used a spatial approach [19]. However, more recent work is using a temporal approach [16, 20].

The motivation behind the work presented here is the modeling of the locomotion dynamics and the design of closed-loop control laws for implementing locomotion in a caterpillar-inspired soft-robot. Recent work by Goldberg et al. [21] applied discrete elastic rod (DER) theory to model the dynamics of a soft robot caterpillar as a discrete rod that can stretch and bend with elastic and stretching energies. The model used planar discrete elastic rod (PDER) in combination with open-loop control to predict the motion of a caterpillar-inspired soft robot [21]. One of the difficulties of designing closed-loop control laws for a soft-robot is model nonlinearity; another is computational complexity.

This work uses a network approach to model a caterpillar's locomotion. The first model consists of a collection of N spring mass damper systems with and without physical coupling. The second model is a collection of N torsional springs of fixed lengths also with and without physical coupling. Each agent is controlled through the rate of change of its rest length (respectively, rate of change of its resting relative angle). The choice of our control variable is motivated by the PDER model, in which stretching and bending energies are functions of intrinsic properties like rest length [21]. The first model exhibits a change of length as the system stretches and compresses, whereas the second model exhibits a change in angle (bending) and angular velocity. In ongoing work, we seek to combine these models and their control to create closed-loop feedback laws applicable to the control of simultaneous bending and stretching.

The contributions of this paper are (1) a network approach to modeling the dynamics of a collection of spring-mass-dampers and torsional springs controlled by the change in intrinsic length or curvature, and (2) the design of closed-loop feedback laws to achieve (a) consensus and (b) traveling wave solution in either model. Simulation results show that high-gain linear controls stabilize the consensus and traveling wave solutions regardless of the initial conditions. However, when applied to the nonlinear system, the same control laws lead to consensus and traveling waves only for initial conditions close to the equilibrium point and for sufficiently large gain values.

The organization of this paper is as follows: Section II of this paper presents a review of graph theory, consensus theory, and the wave equation. Section III introduces the mathematical model and feedback control laws of a network of linked spring-mass-dampers, with controllers designed for consensus and traveling wave behaviors. Section IV repeats the process for a network of linked torsional springs. Section V summarizes the paper and ongoing work.

BACKGROUND

This paper models the actuators of a caterpillar soft robot as modular linear or torsional springs. A network of N actuators is connected in a neighbor-to-neighbor circulant topology. This section presents an overview of graph theory, consensus control, and traveling wave control.

Graph Theory

Consider the undirected graph $\mathcal{G} = (\mathcal{V}, \mathcal{E})$, where $\mathcal{V}$ is the set of N vertices and $\mathcal{E}$ is the set of edges connecting pairs of vertices. The Laplacian matrix $\mathcal{L} = D - A$ defines the communication topology of the network, where the adjacency matrix $A \in \mathbb{R}^{NxN}$ is symmetric, with entries $a_{ij} = a_{ji}$ given by

$$a_{ij} = \begin{cases} 1, & \text{if } i \neq j \quad \text{and } (i,j) \in \mathcal{E} \\ 0, & \text{otherwise.} \end{cases}$$

The degree matrix $D \in \mathbb{R}^{N \times N}$ is defined as

$$d_{ij} = \begin{cases} \sum_{j=1}^{N} a_{ij}, & \text{if } i = j \\ 0, & \text{otherwise.} \end{cases}$$

The Laplacian of an undirected graph is a symmetric, positive semi-definite matrix with zero row sums [22]. For example, the Laplacian matrix of an undirected cyclic graph with degree 2 is

$$\mathcal{L} = \begin{bmatrix} 2 & -1 & 0 & & \cdots & & -1 \\ -1 & 2 & -1 & 0 & \cdots & & 0 \\ 0 & -1 & 2 & -1 & 0 & \cdots & 0 \\ \vdots & \ddots & \ddots & \ddots & \ddots & & \vdots \\ \vdots & & \ddots & \ddots & \ddots & \ddots & \\ \vdots & & & \ddots & -1 & 2 & -1 \\ -1 & 0 & \cdots & & 0 & -1 & 2 \end{bmatrix} \in \mathbb{R}^{N\times N}. \tag{1}$$

Note that Eq. (1) is a circulant matrix, i.e., each row vector is a cyclic permutation of the preceding row vector.

Consensus Control

Consensus is achieved when multiple systems that are connected by local interactions achieve a common behavior [23]. Given a network of N second-order integrators with information states x and $\dot{x}$ and connected to each other through local interactions, consensus is achieved if $\forall\, x_i(0), |x_i(t) - x_j(t)| \to 0$ as $t \to \infty, \forall\, i, j = 1, \ldots, N$ [23, Chapter 4]. Given the systems' individual dynamics, a consensus algorithm can be designed to achieve consensus over the information state through the use of the Laplacian $\mathcal{L}$ matrix of the communication topology associated with the network of systems.As an example, consider the double-integrator dynamics given by $\ddot{x} = -cAx - bB\dot{x} + u$, where $b, c \in \mathbb{R}^+$. Using the consensus algorithm $u = c(A-I)x + b(B-\mathcal{L})\dot{x}$ leads to the closed-loop consensus dynamics $\ddot{x} = -cx - b\mathcal{L}\dot{x}$ [16, 24]. We need the following theorem for our main results.

Theorem 1. *Consider the second-order system*

$$\ddot{x} = -cAx - bF\dot{x} + cA\bar{x} \tag{2a}$$
$$\dot{\bar{x}} = u, \tag{2b}$$

where matrix A is invertible. Let $\mathcal{L}$ be the Laplacian matrix associated with the desired communication topology, such that $\mathcal{L}$ has a simple zero eigenvalue and all other eigenvalues are positive. The feedback control law $u = \gamma((I - A^{-1})x + b/cA^{-1}(F - \mathcal{L})\dot{x} - \bar{x})$, drives the network to achieve consensus over time in position and velocity.

Proof. We know that second-order consensus is achieved by $\ddot{x} = -cx - b\mathcal{L}\dot{x}$ [16, 24]. Setting our second-order dynamics (2a) to equal the desired dynamics, we solve for $\bar{x}_{des} = (I - A^{-1})x + b/cA^{-1}(F - \mathcal{L})\dot{x}$. Define a high-gain controller $u = \gamma(\bar{x}_{des} - \bar{x})$. For $\gamma \gg 1$, $\bar{x} \to \bar{x}_{des}$. In addition, there is a time-scale separation such that the dynamics of x and $\dot{x}$ are slower than that of $\bar{x}$. As a result, our network reduces to the closed-loop form $\ddot{x} = -cx - b\mathcal{L}\dot{x}$, which achieves consensus [16, 24].

Traveling Wave Control

A wave equation is a second-order hyperbolic partial differential equation that can be used to model the displacement of a wave, such as a compressive stress wave in a finite system of spring-mass models [25]. Given the displacement vector $u(x,t)$ of the set of masses where x is the spatial displacement and t is the time, the wave propagation subject to the boundary conditions can be modeled as $u_{tt} + c\Delta u = 0$, where u_{tt} is the second partial derivative of u with respect to t, c is the speed of propagation, and Δ is the Laplace operator [25]. When approximating the infinite length of a thin elastic rod by a set of discrete points such as spring-mass or torsional spring models, Δ is approximated by the Laplacian $\mathcal{L}$ such that the wave propagation dynamics is $\ddot{x} + c\mathcal{L}x = 0$. We need the following theorem for our main results.

Theorem 2. *Consider the second-order system described in Eq. (2) with associated Laplacian matrix $\mathcal{L}$, such that $\mathcal{L}$ has a simple zero eigenvalue and all other eigenvalues are positive. The feedback control law $u = \gamma((I - A^{-1}\mathcal{L})x + b/cA^{-1}F\dot{x} - \bar{x})$, drives the network to exhibit a traveling wave solution.*

Proof. We know that a second-order discretized wave equation is given by $\ddot{x} = -c\mathcal{L}x$ [16]. Setting the second-order dynamics (2a) to equal the desired dynamics yields $\bar{x}_{des} = ((I - A^{-1}\mathcal{L})x + b/cA^{-1}F\dot{x}$. Similar to the proof of Theorem 1, define a high gain controller $u = \gamma(\bar{x}_{des} - \bar{x})$ and use time-scale separation so that the network's dynamics reduce to the closed-loop form $\ddot{x} = -c\mathcal{L}x$, which has a stable traveling wave solution for sufficiently large N [16].

FEEDBACK CONTROL OF LINEAR SPRINGS

This section considers a system of N identical linear damped springs with adjustable rest length connected to masses, first in parallel without physical coupling, then in series with alternating masses and springs connected in a chain. Each spring has a spring constant c_i, damping coefficient b_i, and rest length $\bar{x}_i$, with attached mass m_i, for $i = 1, \ldots, N$. Each spring is controlled through its rate of change of rest length $\dot{\bar{x}}_i = u_i$. We derive the mathematical model and later assume $m = 1$. We then design control laws to achieve consensus and a wave equation.

Consider N spring-mass-damper connected in parallel to a fixed surface as in Fig. 1. The individual dynamics of the spring-mass dampers are $\ddot{x}_i = -c(x_i - \bar{x}_i) - b\dot{x}_i, \dot{\bar{x}}_i = u_i \forall\, i = 1, \ldots, N$. Let $x = (x_1, \ldots, x_N)^T$ be the vector of all the positions. In addition, let $u = (u_1, \ldots, u_N)^T$ be the vector of control inputs. We have

$$\frac{d}{dt}\begin{bmatrix} x \\ \dot{x} \\ \bar{x} \end{bmatrix} = \underbrace{\begin{bmatrix} 0 & I & 0 \\ -cI & -bI & cI \\ 0 & 0 & 0 \end{bmatrix}}_{\triangleq A_s^0} \begin{bmatrix} x \\ \dot{x} \\ \bar{x} \end{bmatrix} + \underbrace{\begin{bmatrix} 0 \\ 0 \\ I \end{bmatrix}}_{\triangleq B_s} u, \tag{3}$$

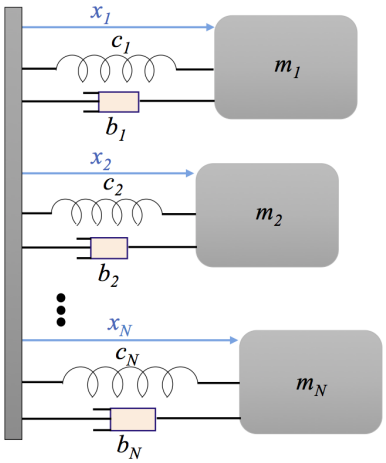

Figure 1. NETWORK OF N SPRING-MASS-DAMPER WITH NO PHYSICAL COUPLING

where I is the $N \times N$ identity matrix. The set of equilibrium points of the autonomous system described in Eq. (3) is continuous, $\{x, \dot{x}, \bar{x} \in \mathbb{R}^N \mid x = \bar{x}, \dot{x} = 0\}$.The system is controllable because the controllability matrix $\mathcal{C} = [B_s \quad A_s^0 B_s \dots (A_s^0)^{N-1} B_s]$ has full rank. Using Theorem 1, consensus is achieved on the position x and the velocity $\dot{x}$ by choosing the control $u = \gamma(\frac{b}{c}(I - \mathcal{L})\dot{x} - \bar{x})$, where $\mathcal{L}$ is the circulant Laplacian defined in Section II. The closed-loop consensus system is

$$\frac{d}{dt}\begin{bmatrix} x \\ \dot{x} \\ \bar{x} \end{bmatrix} = \begin{bmatrix} 0 & I & 0 \\ -cI & -bI & cI \\ 0 & \gamma\frac{b}{c}(I-\mathcal{L}) & -\gamma I \end{bmatrix}\begin{bmatrix} x \\ \dot{x} \\ \bar{x} \end{bmatrix}. \tag{4}$$

Figure 2 shows the consensus dynamics for a network of 4 spring-mass-dampers with no physical coupling.

Following Theorem 2, applying the control $u = \gamma((I - \mathcal{L})x + \frac{b}{c}\dot{x} - \bar{x})$ yields a closed-loop system with traveling wave solution

$$\frac{d}{dt}\begin{bmatrix} x \\ \dot{x} \\ \bar{x} \end{bmatrix} = \begin{bmatrix} 0 & I & 0 \\ -cI & -bI & cI \\ \gamma(I-\mathcal{L}) & \gamma\frac{b}{c}I & -\gamma I \end{bmatrix}\begin{bmatrix} x \\ \dot{x} \\ \bar{x} \end{bmatrix}. \tag{5}$$

Figure 3 shows the traveling wave solution for a network of 10 spring-mass-dampers with no physical coupling, and Gaussian initial position and initial velocity as derivative of the Gaussian distribution.

Next, consider a system of $N+1$ identical masses connected in series to their nearest neighbors via a set of N controlled damped springs. Mass m_{i-1} and m_i are connected via spring i

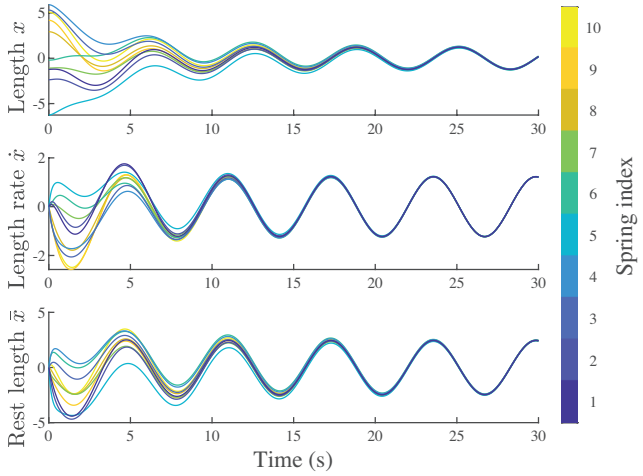

Figure 2. CONSENSUS DYNAMICS FOR SYSTEM OF MASS-SPRING-DAMPERS WITH NO PHYSICAL COUPLING, COLORED BY SPRING INDEX. $N = 10$, $\gamma = 10^5$, $b = 2$, $c = 1$.

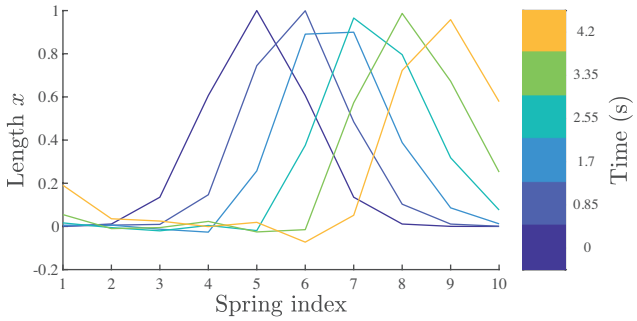

Figure 3. SNAPSHOTS OF TRAVELING WAVE CONTROL FOR A NETWORK OF SPRING-MASS-DAMPERS WITH NO PHYSICAL COUPLING. $N = 10$, $\gamma = 10^5$, $b = 2$, $c = 1$

for $i = 1, \dots, N$. Let $z_i = x_i - x_{i-1}$ for $i = 1, \dots, N$ be the spring lengths, and let $\bar{z}_i$ be the controlled natural length of each spring, with $\dot{\bar{z}}_i = u_i$. Setting all $m_i = 1$, the dynamics are now described by

$$\begin{aligned} \ddot{x}_0 &= k_1(x_1 - x_0 - \bar{z}_1) + b_1(\dot{x}_1 - \dot{x}_0), \\ \ddot{x}_i &= -k_i(x_1 - x_{i-1} - \bar{z}_i) - b_i(\dot{x}_i - \dot{x}_{i-1}) \\ &\quad + k_{i+1}(x_{i+1} - x_i - \bar{z}_{i+1}) + b_{i+1}(\dot{x}_{i+1} - \dot{x}_i),\ i = 1, \dots, N-1 \\ \ddot{x}_N &= -k_N(x_1 - x_{N-1} - \bar{z}_N) - b_N(\dot{x}_N - \dot{x}_{N-1}). \end{aligned} \tag{6}$$

There are no external forces, thus momentum is conserved and there is no net movement of the center of mass. We can write the

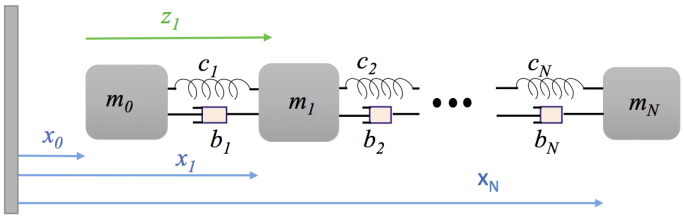

Figure 4. SYSTEM OF N MASS-SPRING-DAMPERS WITH PHYSICAL COUPLING BETWEEN NEIGHBORS.

reduced system of spring length dynamics as

$$\frac{d}{dt}\begin{bmatrix} z \\ \dot{z} \\ \bar{z} \end{bmatrix} = \begin{bmatrix} 0 & I & 0 \\ -cQ & -bQ & cQ \\ 0 & 0 & 0 \end{bmatrix} \begin{bmatrix} z \\ \dot{z} \\ \bar{z} \end{bmatrix} + \begin{bmatrix} 0 \\ 0 \\ I \end{bmatrix} u, \tag{7}$$

where Q is the N-by-N invertible matrix

$$Q = \begin{bmatrix} 2 & -1 & 0 & \cdots & & 0 \\ -1 & 2 & -1 & 0 & \cdots & 0 \\ 0 & -1 & 2 & -1 & \ddots & \\ \vdots & \ddots & \ddots & & \ddots & 0 \\ 0 & \cdots & & -1 & 2 & -1 \\ 0 & \cdots & & 0 & -1 & 2 \end{bmatrix}.$$

As in the previous case, we have a continuum of equilibria, $z = \bar{z} = z^*$, $\dot{z} = 0$, $\forall z^* \in \mathbb{R}^N$. Using Theorem 1, choosing the control input $u = \gamma((I - Q^{-1})z + b/c(I - Q^{-1}\mathcal{L})\dot{z} - \bar{z})$ with $\gamma \gg 0$ leads to consensus between all the spring lengths via the closed loop dynamics

$$\frac{d}{dt}\begin{bmatrix} z \\ \dot{z} \\ \bar{z} \end{bmatrix} = \begin{bmatrix} 0 & I & 0 \\ -cQ & -bQ & cQ \\ \gamma(I - Q^{-1}) & \gamma\frac{b}{c}(I - Q^{-1}\mathcal{L}) & -\gamma I \end{bmatrix} \begin{bmatrix} z \\ \dot{z} \\ \bar{z} \end{bmatrix}. \tag{8}$$

Figure 5 shows the consensus dynamics in a network of 4 spring-mass-dampers with neighbor-to-neighbor physical coupling.

In a similar use of Theorem (2), the control $u = \gamma((I - Q^{-1}\mathcal{L})z + \frac{b}{c}\dot{z} - \bar{z})$ yields a closed-loop system with traveling wave behavior:

$$\frac{d}{dt}\begin{bmatrix} z \\ \dot{z} \\ \bar{z} \end{bmatrix} = \begin{bmatrix} 0 & I & 0 \\ -cQ & -bQ & cQ \\ \gamma\left(I - Q^{-1}\mathcal{L}\right) & \gamma\frac{b}{c}I & -\gamma I \end{bmatrix} \begin{bmatrix} z \\ \dot{z} \\ \bar{z} \end{bmatrix}, \tag{9}$$

Figure 6 shows the traveling wave solution for a network of 10 controlled damped springs coupled in series, using a Gaussian

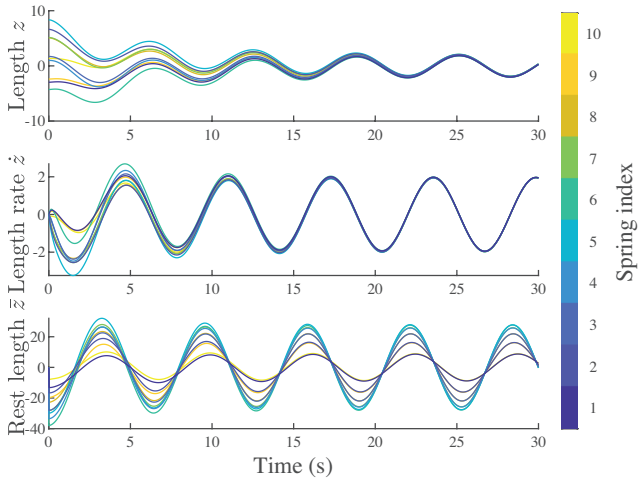

Figure 5. CONSENSUS DYNAMICS FOR LINEAR SYSTEM OF $N = 10$ INPUTS FOR MASS-SPRING-DAMPER SYSTEM WITH PHYSICAL COUPLING BETWEEN NEIGHBORS, COLORED BY SPRING INDEX. $\gamma = 10^5$, $b = 2$, $c = 1$.

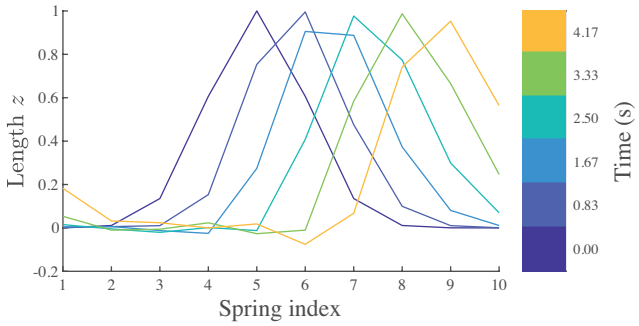

Figure 6. SNAPSHOTS OF TRAVELING WAVE CONTROL FOR SPRING MASS DAMPER WITH PHYSICAL COUPLING. $N = 10$, $\gamma = 10^5$, $b = 2$, $c = 1$.

initial position and initial velocity as derivative of the Gaussian distribution.

FEEDBACK CONTROL OF TORSIONAL SPRINGS

This section applies the framework defined in the previous section to damped torsional springs with control of the rate of change of the resting angle. We first consider a system of N springs each attached at one end to a fixed surface and at the other end to a massless rod of length l tipped with a point mass m, illustrated in Fig. 7. Next we consider a coupled chain of

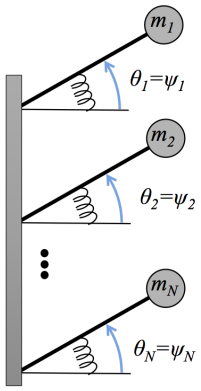

Figure 7. SYSTEM OF N TORSIONAL SPRINGS WITH NO PHYSICAL COUPLING.

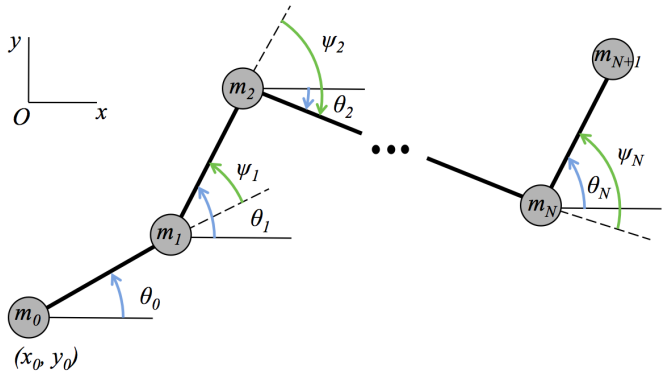

Figure 8. SYSTEM OF N TORSIONAL SPRINGS WITH PHYSICAL COUPLING BETWEEN NEIGHBORS.

$N+2$ masses and $N+1$ rods alternating in a series, with N of the torsional springs attached at each mass except the ends, shown in Fig. 8. We define the displacement angles of the springs as ψ_i, the controlled resting angles as $\bar{\psi}_i$, with velocity inputs $\dot{\bar{\psi}}_i = u_i$ for $i = 1,\ldots,N$. Additionally, each spring is damped with damping coefficient ζ. The system is not subject to gravitational energy.

We define the elastic energy contained in the torsional springs based on the planar discrete elastic rod model of [21], where the bending energy in each node of a discrete rod is proportional to the square of the change in discrete curvature, defined $\kappa_i = 2\tan(\psi_i/2)$. For the torsional spring system, the bending energy for spring i is

$$E_{spring,i} = \frac{EI}{l}\left(2\tan\left(\frac{\psi_i}{2}\right) - 2\tan\left(\frac{\bar{\psi}_i}{2}\right)\right)^2, \qquad (10)$$

where EI is the bending stiffness, or flexural rigidity, of the rod [26]. In the non-coupled configuration, the kinetic energy of each mass is $T_i = ml^2\dot{\psi}_i^2$. Using the Euler-Lagrange equations [27], and setting $m = 1$, the dynamics of each damped torsional spring is

$$\ddot{\psi}_i = -\frac{2EI}{l^3}(\tan\frac{\psi_i}{2} - \tan\frac{\bar{\psi}_i}{2})(\tan^2\frac{\psi_i}{2} + 1) - \frac{\zeta}{l^2}\dot{\psi}_i, \qquad (11)$$

defined for $\psi_i \in (-\pi,\pi)$. The continuous range of equilibria of the system are in the form $\psi = \bar{\psi} = \psi^*$, $\dot{\psi} = 0$, $\forall \psi^* \in \mathbb{R}^N$. The dynamics of N torsional springs, linearized about an arbitrary equilibrium point yields the $3N \times 1$ state space system

$$\frac{d}{dt}\begin{bmatrix}\psi'\\ \dot{\psi}\\ \bar{\psi}'\end{bmatrix} = \begin{bmatrix}0 & I & 0\\ -cG & -bI & cG\\ 0 & 0 & 0\end{bmatrix}\begin{bmatrix}\psi'\\ \dot{\psi}\\ \bar{\psi}'\end{bmatrix} + \begin{bmatrix}0\\ 0\\ I\end{bmatrix}u, \qquad (12)$$

where $c = \frac{EI}{l^3}$, $b = \frac{\zeta}{l^2}$, I is the $N \times N$ identity matrix,

$$G = \begin{bmatrix}\xi_0 & 0 & \cdots & 0\\ 0 & \xi_1 & 0 & \vdots\\ \vdots & \ddots & \ddots & \\ 0 & \cdots & & \xi_{N-1}\end{bmatrix} \in \mathbb{R}^{N\times N},$$

and $\xi_i = \tan^2\frac{\psi_i^*}{2} + 1$, with $\psi' = \psi - \psi^*$, $\bar{\psi}' = \bar{\psi} - \psi^*$ defining the equilibrium.

In particular, when the equilibrium point is at the origin $\psi^* = 0$, the system's dynamics become

$$\frac{d}{dt}\begin{bmatrix}\psi\\ \dot{\psi}\\ \bar{\psi}\end{bmatrix} = \begin{bmatrix}0 & I & 0\\ -cI & -bI & cI\\ 0 & 0 & 0\end{bmatrix}\begin{bmatrix}\psi\\ \dot{\psi}\\ \bar{\psi}\end{bmatrix} + \begin{bmatrix}0\\ 0\\ I\end{bmatrix}u. \qquad (13)$$

This system is equivalent to the linear spring-mass-damper network with no physical coupling and control laws for this particular case are identical.

Next, consider a system of $N+2$ point masses (labeled 0 through $N+1$) in the plane connected to the nearest neighbor masss via $N+1$ massless rods of length l (labeled 0 through N) (see Fig. 8). The configuration of the system is given by $q = (x_0, y_0, \theta_0, ..., \theta_n)^T$, where x_0 and y_0 are the location of mass m_0 in an inertial coordinate system, and θ_i is the absolute orientation of edge i connecting mass i to mass $i+1$ measured counterclockwise from the x-axis. We affix a torsional spring to each mass (excluding the ends) such that the elastic stored energy is given by Eq. (10) with spring displacement defined as the turning angles $\psi_i = \theta_i - \theta_{i-1}$ for $i = 1, ..., N$.

The inertial locations of the masses are

$$x_i = x_0 + l\sum_{j=0}^{i-1}\cos\theta_j,\ i=1,...,N+1$$
$$y_i = y_0 + l\sum_{j=0}^{i-1}\sin\theta_j,\ i=1,...,N+1$$

and their velocities are

$$\dot{x}_i = \dot{x}_0 - l\sum_{j=0}^{i-1}\dot{\theta}_j\sin\theta_j,\ i=1,...,N+1$$
$$\dot{y}_i = \dot{y}_0 + l\sum_{j=0}^{i-1}\dot{\theta}_j\cos\theta_j,\ i=1,...,N+1$$

We derive equations of motion via the Euler-Lagrange equations, with Lagrangian $L = \frac{1}{2}m\sum_{i=0}^{N+1}(\dot{x}_i^2+\dot{y}_i^2) - \sum_{j=1}^{N}E_j$.

$$\frac{\partial L}{\partial \dot{x}} = m\sum_{i=0}^{N+1}\dot{x}_i\frac{\partial \dot{x}_i}{\partial \dot{x}} = m(N+2)\dot{x} - ml\sum_{i=1}^{N+1}\sum_{j=0}^{i-1}\dot{\theta}_j\sin\theta_j \quad (14)$$

$$\frac{\partial L}{\partial \dot{y}} = m\sum_{i=0}^{N+1}\dot{y}_i\frac{\partial \dot{y}_i}{\partial \dot{y}} = m(N+2)\dot{y} + ml\sum_{i=1}^{N+1}\sum_{j=0}^{i-1}\dot{\theta}_j\cos\theta_j \quad (15)$$

Variables x and y are cyclic, associated with the conservation of the total linear momentum of the system. Defining p_x and p_y as the constant linear momenta along the x and y axes, we have

$$\dot{x}_0 = \frac{1}{m(N+2)}\left(p_x + ml\sum_{i=1}^{N+1}\sum_{j=0}^{i-1}\dot{\theta}_j\sin\theta_j\right),$$
$$\dot{y}_0 = \frac{1}{m(N+2)}\left(p_y - ml\sum_{i=1}^{N+1}\sum_{j=0}^{i-1}\dot{\theta}_j\cos\theta_j\right), \quad (16)$$

Since we are primarily concerned with controlling the shape of the rod, we substitute for $\dot{x}_0$ and $\dot{y}_0$ in the Langrangian to form a reduced Lagrangian for the angle dynamics: $L_r = L_r(\theta,\dot{\theta},\bar{\psi})$. The equations of motion for the reduced system are

$$\frac{d}{dt}\left(\frac{\partial L_r}{\partial \dot{\theta}_i}\right) - \frac{\partial L_r}{\partial \theta} = 0,\ i=0,...,N, \quad (17)$$

which take the standard form

$$M(\theta)\ddot{\theta} + C(\theta,\dot{\theta}) + V(\theta) = 0. \quad (18)$$

For convenience, define a matrix of coefficients with entries

$$a_{ij} = (k+1)(N+1-k-|i-j|),\ \text{where}\ k = \min\{i,j,N-i,N-j\}, \quad (19)$$

for $i,j\in\{0,...,N\}$. Then entries of the mass matrix $M(\theta)$ are

$$M_{ij} = a_{ij}\frac{ml^2}{N+2}\cos(\theta_i-\theta_j), \quad (20)$$

and entries of the gyroscopic term $C(\theta,\dot{\theta})$ are

$$C_i = \frac{ml^2}{N+2}\sum_{j=0}^{N}a_{ij}\dot{\theta}_j(\dot{\theta}_i-\dot{\theta}_j)\sin(\theta_j-\theta_i). \quad (21)$$

Finally, the terms due to spring forces $V(\theta,\bar{\psi})$ are

$$V_i = \quad (22)$$
$$\begin{cases} -\frac{2EI}{l}\sec^2\left(\frac{\theta_1-\theta_0}{2}\right)\left(\tan\left(\frac{\theta_1-\theta_0}{2}\right)-\tan(\bar{\psi}_1/2)\right), i=0 \\ \frac{2EI}{l}\sec^2\left(\frac{\theta_i-\theta_{i-1}}{2}\right)\left(\tan\left(\frac{\theta_i-\theta_{i-1}}{2}\right)-\tan(\bar{\psi}_i/2)\right) \\ \quad -\frac{2EI}{l}\sec^2\left(\frac{\theta_{i+1}-\theta_i}{2}\right)\left(\tan\left(\frac{\theta_{i+1}-\theta_i}{2}\right)-\tan(\bar{\psi}_{i+1}/2)\right), \\ \quad \forall\quad 0<i<N, \\ \frac{2EI}{l}\sec^2\left(\frac{\theta_N-\theta_{N-1}}{2}\right)\left(\tan\left(\frac{\theta_N-\theta_{N-1}}{2}\right)-\tan(\bar{\psi}_N/2)\right), \\ \quad i=N. \end{cases}$$

Linearizing about the equilibrium ($\theta=0$, $\dot{\theta}=0$, $\bar{\psi}=0$), we find that the system matrices have a banded structure, i.e.,

$$\ddot{\theta} = \frac{EI}{ml^3}A\theta + \frac{EI}{ml^3}B\bar{\psi}, \quad (23)$$

where

$$A = \begin{bmatrix} -3 & 4 & -1 & & & & 0 \\ 3 & -6 & 4 & -1 & & & \\ -1 & 4 & -6 & 4 & -1 & & \\ & \ddots & \ddots & \ddots & \ddots & \ddots & \\ & & -1 & 4 & -6 & 4 & -1 \\ & & & -1 & 4 & -6 & 3 \\ 0 & & & & -1 & 4 & -3 \end{bmatrix}, \quad (24)$$

and

$$B = \begin{bmatrix} -3 & 1 & & & 0 \\ 3 & -3 & 1 & & \\ -1 & 3 & -3 & 1 & \\ & \ddots & \ddots & \ddots & \ddots \\ & & -1 & 3 & -3 & 1 \\ & & & -1 & 3 & -3 \\ 0 & & & & -1 & 3 \end{bmatrix} \tag{25}$$

There remains an uncontrollable mode in the linearized system, which is associated with the rotational symmetry of the rod. We introduce the following coordinate transformation to isolate the controllable states, the relative angles between edges, ψ_i:

$$\begin{bmatrix} \theta_0 \\ \psi \end{bmatrix} = \begin{bmatrix} 1 & & 0 \\ -1 & 1 & \\ & \ddots & \ddots \\ 0 & & -1 \; 1 \end{bmatrix} \theta. \tag{26}$$

The reduced, controllable linearized system is

$$\ddot{\psi} = \frac{EI}{ml^3} H(\bar{\psi} - \psi). \tag{27}$$

with the banded matrix

$$H = \begin{bmatrix} 6 & -4 & 1 & & 0 \\ -4 & \ddots & \ddots & \ddots & \\ 1 & \ddots & \ddots & \ddots & 1 \\ & \ddots & \ddots & \ddots & -4 \\ 0 & & 1 & -4 & 6 \end{bmatrix} \tag{28}$$

Applying Theorem 1, the input control to the linearized system $u = \gamma((I - H^{-1})\psi - \frac{b}{c} H^{-1} \mathcal{L} \dot{\psi} - \bar{\psi})$ leads to the linear consensus form with $c = \frac{EI}{ml^3}$. The linearized closed-loop consensus system is

$$\frac{d}{dt} \begin{bmatrix} \psi \\ \dot{\psi} \\ \bar{\psi} \end{bmatrix} = \begin{bmatrix} 0 & I & 0 \\ -cH & 0 & cH \\ \gamma(I - H^{-1}) & -\gamma \frac{b}{c} H^{-1} \mathcal{L} & -\gamma I \end{bmatrix} \begin{bmatrix} \psi \\ \dot{\psi} \\ \bar{\psi} \end{bmatrix}, \tag{29}$$

and the nonlinear closed-loop consensus system is

$$\frac{d}{dt} \begin{bmatrix} \theta \\ \dot{\theta} \\ \bar{\psi} \end{bmatrix} = \begin{bmatrix} \dot{\theta} \\ -M(\theta)^{-1} \left(V(\theta) + C(\theta, \dot{\theta}) \right) \\ \gamma \left((I - H^{-1}) \psi - \frac{b}{c} H^{-1} \mathcal{L} \dot{\psi} - \gamma \bar{\psi} \right) \end{bmatrix}. \tag{30}$$

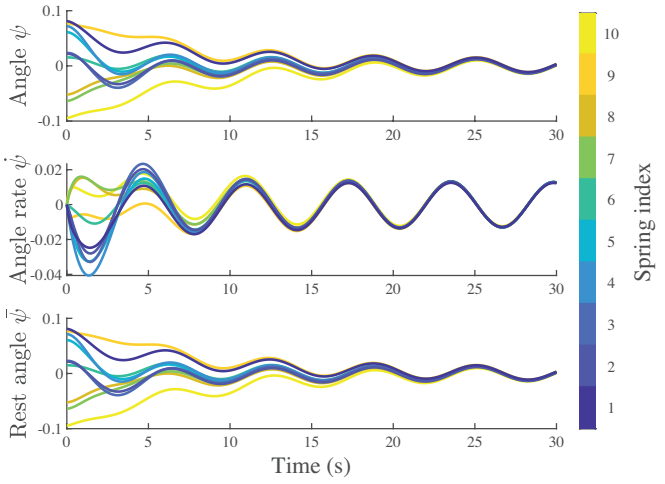

Figure 9. LINEAR CONSENSUS CONTROL APPLIED TO NONLINEAR SYSTEM OF N TORSIONAL SPRINGS WITH PHYSICAL COUPLING. $N = 10$ INPUTS, $\gamma = 10^5$, $b = 2$, $c = 1$.

Figure 9 shows consensus dynamics for a system of undamped torsional springs with 4 inputs and nonlinear dynamics, controlled by a linear feedback and with initial conditions $\psi(0)$ chosen randomly between the range $(-0.2, 0.2)$.

In a similar way, using Theorem 2 and applying the linear control $u = \gamma((I - H^{-1}\mathcal{L})\psi - \bar{\psi})$ to the linearized system yields the closed-loop system that achieves a traveling wave solution:

$$\frac{d}{dt} \begin{bmatrix} \psi \\ \dot{\psi} \\ \bar{\psi} \end{bmatrix} = \begin{bmatrix} 0 & I & 0 \\ -cH & 0 & cH \\ \gamma(I - H^{-1}\mathcal{L}) & 0 & -\gamma I \end{bmatrix} \begin{bmatrix} \psi \\ \dot{\psi} \\ \bar{\psi} \end{bmatrix}. \tag{31}$$

The nonlinear closed-loop traveling wave system is

$$\frac{d}{dt} \begin{bmatrix} \theta \\ \dot{\theta} \\ \bar{\psi} \end{bmatrix} = \begin{bmatrix} \dot{\theta} \\ -M(\theta)^{-1} \left(V(\theta) + C(\theta, \dot{\theta}) \right) \\ \gamma \left((I - H^{-1}\mathcal{L})\psi - \bar{\psi} \right) \end{bmatrix}, \tag{32}$$

where M, C, and V are given by Eqs. (20)-(22).

Figure 10 shows the traveling wave solution for the nonlinear system of 10 torsional springs and initial angle as Gaussian distribution and velocity set as derivative of the Gaussian.

CONCLUSION

A caterpillar's crawling gait exhibits traveling wave propagating from tail to head. We modeled a caterpillar soft robot using a network of linear and torsional springs. Using the change in

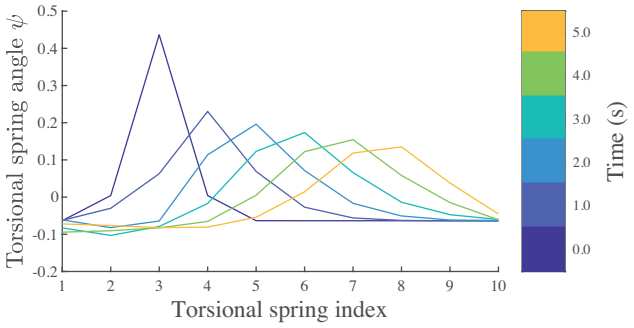

Figure 10. LINEAR TRAVELING WAVE CONTROL APPLIED TO NONLINEAR SYSTEM OF N TORSIONAL SPRINGS WITH PHYSICAL COUPLING. $N = 10$ INPUTS, $\gamma = 100000$, $c = 1$.

the intrinsic length and curvature as input, we designed closed-loop feedback control laws stabilize consensus and traveling wave solutions. Ongoing work combines linear and torsional spring models and their control laws to achieve account for bending and stretching in a caterpillar-inspired soft-robot.

ACKNOWLEDGMENT

We thank Travis Burch for discussions related to this paper.

REFERENCES

[1] Trimmer, B. A., Takesian, A. E., Sweet, B. M., Rogers, C. B., Hake, D. C., and Rogers, D. J., 2006. "Caterpillar locomotion: a new model for soft-bodied climbing and burrowing robots". In 7th International Symposium on Technology and the Mine Problem, Vol. 1, Monterey, CA: Mine Warfare Association, pp. 1–10.

[2] Trimmer, B. A., 2008. "New challenges in biorobotics: incorporating soft tissue into control systems". *Applied Bionics and Biomechanics,* ***5***(3), pp. 119–126.

[3] Tawk, C., in het Panhuis, M., Spinks, G. M., and Alici, G., 2018. "Bioinspired 3D printable soft vacuum actuators for locomotion robots, grippers and artificial muscles". *Soft Robotics,* ***5***(6), pp. 685–694.

[4] Wehner, M., Truby, R. L., Fitzgerald, D. J., Mosadegh, B., Whitesides, G. M., Lewis, J. A., and Wood, R. J., 2016. "An integrated design and fabrication strategy for entirely soft, autonomous robots". *Nature,* ***536***(7617), pp. 451–455.

[5] Saunders, F., Golden, E., White, R. D., and Rife, J., 2011. "Experimental verification of soft-robot gaits evolved using a lumped dynamic model". *Robotica,* ***29***(6), pp. 823–830.

[6] Shepherd, R. F., Ilievski, F., Choi, W., Morin, S. A., Stokes, A. A., Mazzeo, A. D., Chen, X., Wang, M., and Whitesides, G. M., 2011. "Multigait soft robot". *Proceedings of the National Academy of Sciences,* ***108***(51), pp. 20400–20403.

[7] Wang, W., Wang, K., and Zhang, H., 2009. "Crawling gait realization of the mini-modular climbing caterpillar robot". *Progress in Natural Science,* ***19***(12), pp. 1821–1829.

[8] Umedachi, T., Shimizu, M., and Kawahara, Y., 2019. "Caterpillar-inspired crawling robot using both compression and bending deformations". *IEEE Robotics and Automation Letters,* ***4***(2), pp. 670–676.

[9] Umedachi, T., Vikas, V., and Trimmer, B. A., 2013. "Highly deformable 3-d printed soft robot generating inching and crawling locomotions with variable friction legs". In 2013 IEEE/RSJ International Conference on Intelligent Robots and Systems, IEEE, pp. 4590–4595.

[10] Rogóż, M., Zeng, H., Xuan, C., Wiersma, D. S., and Wasylczyk, P., 2016. "Light-driven soft robot mimics caterpillar locomotion in natural scale". *Advanced Optical Materials,* ***4***(11), pp. 1689–1694.

[11] Zeng, H., Wani, O. M., Wasylczyk, P., and Priimagi, A., 2018. "Light-driven, caterpillar-inspired miniature inching robot". *Macromolecular Rapid Communications,* ***39***(1), p. 1700224.

[12] Lin, H.-T., Leisk, G. G., and Trimmer, B., 2011. "GoQBot: a caterpillar-inspired soft-bodied rolling robot". *Bioinspiration & Biomimetics,* ***6***(2), p. 026007.

[13] Saunders, F., Trimmer, B. A., and Rife, J., 2010. "Modeling locomotion of a soft-bodied arthropod using inverse dynamics". *Bioinspiration & biomimetics,* ***6***(1), p. 016001.

[14] Saunders, F., Golden, E., White, R. D., and Rife, J., 2011. "Experimental verification of soft-robot gaits evolved using a lumped dynamic model". *Robotica,* ***29***(6), pp. 823–830.

[15] Schuldt, D. W., Rife, J., and Trimmer, B., 2015. "Template for robust soft-body crawling with reflex-triggered gripping". *Bioinspiration & biomimetics,* ***10***(1), p. 016018.

[16] Nguewou-Hyousse, H., Franchi, G., and Paley, D. A., 2018. "Microfluidic circuit dynamics and control for caterpillar-inspired locomotion in a soft robot". In 2018 IEEE Conference on Control Technology and Applications (CCTA), IEEE, pp. 286–293.

[17] Umedachi, T., Takeda, K., Nakagaki, T., Kobayashi, R., and Ishiguro, A., 2010. "Fully decentralized control of a soft-bodied robot inspired by true slime mold". *Biological Cybernetics,* ***102***(3), pp. 261–269.

[18] Umedachi, T., and Trimmer, B. A., 2016. "Autonomous decentralized control for soft-bodied caterpillar-like modular robot exploiting large and continuum deformation". In 2016 IEEE/RSJ International Conference on Intelligent Robots and Systems, IEEE, pp. 292–297.

[19] Paley, D. A., Leonard, N. E., Sepulchre, R., Grunbaum, D., and Parrish, J. K., 2007. "Oscillator models and collective motion". *IEEE Control Systems Magazine,* ***27***(4), pp. 89–105.

[20] Zhao, Y., Duan, Q., Wen, G., Zhang, D., and Wang, B., 2018. "Time-varying formation for general linear multiagent systems over directed topologies: A fully distributed adaptive technique". *IEEE Transactions on Systems, Man, and Cybernetics: Systems*.

[21] Goldberg, N. N., Huang, X., Majidi, C., Novelia, A., O'Reilly, O. M., Paley, D. A., and Scott, W. L., 2019. "On planar discrete elastic rod models for the locomotion of soft robots". *Soft Robotics*.

[22] Godsil, C., and Royle, G. F., 2001. *Algebraic graph theory*. Springer, New York.

[23] Ren, W., and Beard, R. W., 2008. *Distributed consensus in multi-vehicle cooperative control*. Springer-Verlag, London.

[24] Ren, W., 2008. "Synchronization of coupled harmonic oscillators with local interaction". *Automatica,* ***44***(12), pp. 3195–3200.

[25] Achenbach, J., 1973. *Wave propagation in elastic solids*. Elsevier.

[26] Carrera, E., Giunta, G., and Petrolo, M., 2011. *Beam structures: classical and advanced theories*. John Wiley & Sons.

[27] Goldstein, H., Poole, C., and Safko, J., 2002. *Classical mechanics*, 3rd ed. Adison Wesley, San Francisco.